CONF--750935--3

Fast Neutron Spectrum and Dosimetry Studies in the Coupled Fast Reactivity Measurements Facility†

J W Rogers, Y. D. Harker, D. A. Millsap

Aerojet Nuclear Company
Idaho National Engineering Laboratory
Idaho Falls, Idaho 83401 USA

Introduction

The fast neutron spectrum of the Coupled Fast Reactivity Measurements Facility (CFRMF) at the Idaho National Engineering Laboratory (INEL) is being used to study and standardize fast reactor neutron dosimetry materials and methods[1,2]. The CFRMF has been designated a "benchmark experiment" to test the cross section data of dosimetry materials as well as other materials used and produced in fast reactors. Information about the neutron energy spectrum of this neutron field is of foremost importance for these applications.

The CFRMF is a zoned-core critical assembly with a fast neutron spectrum zone in the center of an enriched ^{235}U, water moderated thermal "driver" zone[2]. The CFRMF was chosen for these studies because it has a neutron energy spectrum similar to a fast reactor, highly reproducible flux levels with sufficient magnitude for most reaction rate measurements and physical accessibility favorable for most types of dosimetry experiments and neutron spectrometry.

†Work performed under the auspices of the US Energy Research and Development Administration.

In the effort to characterize the CFRMF spectrum standard calculational techniques have been applied using transport, Monte Carlo and resonance theory computerized methods. Also, measurements using established methods of in-core neutron spectrometry have been conducted. The proton recoil method with gas filled detectors, the charged particle method with ^{6}Li semiconductor sandwich detectors and the reaction cross section dependent activation method with multiple foil activation detectors have been used.

The calculated spectrum has been studied to test its sensitivity to model, theory, cross-section data and source distribution.[2] It appears the optimum model and energy group structure has been attained with existing capabilities and any significant changes in spectral shape will be the result of changes in the basic nuclear data. Tests by measured spectral indices show the CFRMF spectrum has no thermal or low energy neutron components due to streaming from the ends of the fast zone. The spectrometry measurements are studied in terms of the merits of each related to cross-sections, efficiency, techniques and analyses. Comparisons of the spectrometry measurements and calculations are made and how portions of the spectrum can be adjusted by these measurements is discussed. Measured reaction rates are compared with calculated reaction rates of dosimetry materials using various forms of the CFRMF spectrum derived from calculations, calculations adjusted by spectrometry measurements and calculations adjusted by reaction rate measurements and reaction cross sections. All of these approaches tend to, in general, give better agreement between measured and calculated reaction rates.

Calculations

The neutron energy spectrum of CFRMF as calculated by computer codes has been used for the testing of dosimetry cross section data files. This spectrum was derived from a cylindrical model, one-dimensional S_n transport code calculation using ENDF/B Version III cross section data[2] and is shown in Figure 1. A Monte Carlo calculation with pointwise cross-section data was made to test for smoothing effects that may have occurred due to the cross-section processing. The latter calculation covered the energy region from 15 keV to 10 MeV and a comparison of the two spectra is shown in Figure 2. The differences indicated there resulted in no significant changes (< 1%) in calculated reaction rates of $^{235}U(n,f)$, $^{238}U(n,f)$ and $^{197}Au(n,\gamma)$. Resonance absorption calculations between 50 keV and 1 eV generated group fluxes that are compared to the transport spectrum in Figure 3. Again the $^{235}U(n,f)$ and $^{197}Au(n,\gamma)$ reactions were not changed significantly (< 1%).

Extensive tests of the cylindrical model to give the best representation of the complex CFRMF assembly have been conducted.[2] The best compromise between neutron energy group structure and material regions within the computer core storage limitations allows 69 energy groups with 0.25 lethargy spacing and an upper energy of 10 MeV.

These calculations have all used ENDF/B Version III cross sections. Conversion to the Version IV cross sections is nearly completed. The change made in Version IV data that is expected to significantly affect the calculated spectrum is the ^{238}U inelastic scattering cross section. The best calculated spectrum for CFRMF currently available is given in Table I. This spectrum will be used as a reference spectrum in comparisons with measurements in the following sections and will be referred to as the benchmark spectrum.

Integral Spectral Indices Tests

Measurements of the reaction rates of $^{235}U(n,f)$ and $^{197}Au(n,\gamma)$ with the foils Cd covered and bare showed no differences indicating that the central test region CFRMF spectrum has no thermal energy component. Measurements of the reaction rates of $^{235}U(n,f)$ and $^{197}Au(n,\gamma)$ with the ends of the CFRMF plugged with ^{10}B and unplugged showed no differences indicating there is no streaming of low energy neutrons into the central test region spectrum from the ends of the assembly.

Proton Recoil Measurements

The spectrum of CFRMF has been measured twice by the proton recoil method. The first series of measurements was made using two detectors, one predominatly hydrogen filled, the other methane filled. Pulse shape analysis (rise-time)[2] was used to discriminate against gamma events so that the applied energy ranges of these two detectors were extended to lower neutron energies and the lower limit of the methane detector overlapped the upper limit of the hydrogen detector. The second series of measurements was made using five detectors, three predominatly hydrogen filled and two methane filled. Gas pressure was used as the parameter to discriminate against gamma events and also to cover neutron energy ranges with energy overlap between detectors of different pressures.[3] The cylindrical detectors are described in Table II. Figure 4 shows the proton recoil measurements compared to the benchmark spectrum. The spectra are scaled in magnitude to be equal at 500 keV. The measurements using pulse shape discrimination against gamma rays show much more structure than the measurements using gas pressure discrimination. There also appears to be an energy shift between the measurements. The reasons for these discrepancies are under investigation. There may have been some unrecognized pulse pile up effects or incorrect gamma subtractions (or both) to cause some of the structure in the pulse shape discrimination measurements. In the pulse shape discrimination measurements the calibration was done at one location and the measurements at another and even though a pulser check showed no electronics gain shifts, it was not possible to check the gas amplification (bias voltage) during the measurements. During the gas pressure discrimination measurements the energy calibration was checked prior to and after each measurement and no shifts were observed. Because of these problems it seems that at this time more credibility can be given to the gas pressure discrimination measurements. These measurements show more flux between 1 MeV and 2 MeV than the benchmark spectrum.

^{6}Li Semiconductor Sandwich Measurements

The CFRMF spectrum has been measured with two ^{6}Li semiconductor sandwich detectors, one with 2π geometry where the diodes are separated by 0.24 mm and the other with energy independent collimation geometry where the diodes are separated by 10 mm[4]. Figure 5 is a sketch of these detector assemblies. Figure 6 is a comparison of the 2π geometry measurement with the benchmark spectrum. The spectra are scaled to be equal in magnitude at 500 keV. Good agreement between these measurements and the benchmark spectrum is observed between 20 keV and 100 keV and also between 500 keV and 7 MeV. Between 100 keV and 500 keV there is a large difference between the ^{6}Li results and the benchmark spectrum or the proton recoil

measurements. The maximum difference occurs at the peak of the ^{6}Li resonance near 250 keV which may imply difficulties in analyzing the measurements over the resonance. The ^{6}Li measured spectrum agrees well with the benchmark spectrum between 1 MeV and 2 MeV where the proton recoil measurements indicated higher flux.

The collimated geometry ^{6}Li measurement agrees with the 2π measurement between 20 keV and 150 keV and between 500 keV and 3.5 MeV. Between 150 keV and 200 keV they disagree with each other as well as with the proton recoil measurements and the benchmark spectrum. The ^{6}Li results are preliminary and further analyses may alter the apparent discrepancies.

Multifoil Activation Analyses

The integral reaction rates of many dosimetry materials have been measured in the CFRMF spectrum in the effort to develop and test dosimetry methods and cross sections.[1] The CFRMF spectrum has been unfolded from a selected group of these integral reaction rates using the respective differential cross section data from ENDF/B Version IV dosimetry file with the benchmark spectrum as the initial guess and two unfolding routines, SAND II[1] and a semi-empirical spectrum model[5]. Figure 7 shows a comparison of these spectra and the benchmark spectrum where the fluxes have been normalized to unity based on the calculated integral reaction rates. The multifoil derived spectra and the benchmark spectrum were used to calculate the reaction rates that have been measured in CFRMF and these calculated values are compared to the measured reaction rates in Table IV. It is clearly seen that this type of analysis can adjust the benchmark spectrum to where the resulting reaction rates agree with the measurements.

Discussion

Calculation by physical theories and data is the only independent method of obtaining an approximation of the CFRMF neutron spectrum over its entire energy range. The complexity of the assembly makes one dimensional transport theory the most practical calculational method but fine energy group structure is limited by computer capabilities. It appears that the optimum model and energy structure has been attained with existing capabilities. Further refinement of the calculated spectrum will result primiarly from the use of more accurate basic nuclear data. An estimate of the uncertainties on the calculated spectrum obtained by propagation of the errors in the data through the computations will present a formidable task that will also likely be limited by computer capability. Some further consideration of multi-dimensional calculations may be taken if necessary to aid in the interpretation of measurements.

Measurements of the CFRMF spectrum by spectrometry methods have been conducted over the 10 keV to 7 MeV energy range with proton recoil [H(n,p)] and charged particle [$^{6}Li(n,\alpha)T$] methods. In the energy ranges where these cross sections are known to ±1 to ±10%, the measured spectra agree in shape with the calculated spectrum if questionable measurements are rejected. If the questionable measurements are not rejected, serious discrepancies exist between measurements and between measurements and calculations. More study of the measurements and analyses will hopefully resolve these discrepancies.

If one accepts the proton recoil measurements by gas pressure discrimination between 65 keV and 2 MeV, the ^{6}Li measurements between 10 keV and 100 keV and between 500 keV and 7 MeV and normalizes these measurements to the benchmark spectrum over these energy ranges, some adjustments to the benchmark spectrum can be made based on measurements. Adjustments between 12 keV and 65 keV based on the ^{6}Li triton analyses data, between 65 keV and 1.7 MeV based on the proton recoil data and between 1.7 MeV and 7 MeV based on the ^{6}Li sum analyses data have been applied to the benchmark spectrum. These adjustments are listed by groups in Table III and are shown in Figure 8. Table IV includes the comparisons of measured-to-calculated reaction rates for this measurements adjusted benchmark spectrum. This measurements adjusted benchmark spectrum brings nearly all the calculated reactions into better agreement with the measured reaction rates except for the very high energy threshold reactions of $^{27}Al(n,p)$ and (n,α).

Both the SAND II and Semi-Empirical adjustment routines are useful as indicators of what the spectrum may be in areas where emphasis is required.

References

[1] McELROY, W. N., KELLOGG, L. S., Nuclear Technology 25, 2 (1975) 130.
[2] ROGERS, J W, MILLSAP, D. A., HARKER, Y. D., Nuclear Technology 25, 2, (1975) 330.
[3] ROGERS, J W, Nuclear Technology Division Annual Progress Report, ANCR-1255 (1975) (to be published).
[4] DeLEEUW, G. and S., "Neutron Spectrometry", this symposium (1975).
[5] HARKER, Y. D., Nuclear Technology Division Annual Progress Report, ANCR-1255 (1975) (to be published).

Table I

CFRMF Central Fluxes as Calculated by SCAMP

One Dimensional Transport, P1-S6 Approximation,
Twenty Region Cell Calculation

SCAMP 73/008

Group Number	Lower Lethargy	Lower Energy (eV)	Real Flux $\phi(u)\Delta u$
1	0.25	7.79×10^6	0.015915
2	0.50	6.07	0.047192
3	0.75	4.72	0.099282
4	1.00	3.68	0.15826
5	1.25	2.87	0.22956
6	1.50	2.23	0.30044
7	1.75	1.74	0.32838
8	2.00	1.35	0.37165
9	2.25	1.05	0.48196
10	2.50	8.21×10^5	0.65123
11	2.75	6.39	0.87768
12	3.00	4.98	1.00
13	3.25	3.88	0.96504
14	3.50	3.02	0.97404
15	3.75	2.35	0.87086
16	4.00	1.83	0.73469
17	4.25	1.43	0.59642
18	4.50	1.11	0.53875
19	4.75	8.65×10^4	0.41965
20	5.00	6.74	0.39890
21	5.25	5.25	0.27323
22	5.50	4.09	0.22890
23	5.75	3.18	0.15576
24	6.00	2.48	0.15655
25	6.25	1.93	0.11410
26	6.50	1.50	0.080494
27	6.75	1.17	0.077870
28	7.00	9.12×10^3	0.065567
29	7.25	7.10	0.051764
30	7.50	5.53	0.044402
31	7.75	4.31	0.042918
32	8.00	3.36	0.043315
33	8.25	2.61	0.034658
34	8.50	2.04	0.031480
35	8.75	1.59	0.033850
36	9.00	1.23×10^3	0.027442
37	9.25	961.1	0.020435
38	9.50	748.5	0.020955
39	9.75	582.9	0.015951
40	10.00	454.0	0.015354
41	10.25	353.6	0.010261
42	10.50	275.4	8.7379×10^{-3}
43	10.75	214.5	6.5036×10^{-3}

Table I (Continued)

Group Number	Lower Lethargy	Lower Energy (eV)	Real Flux $\phi(u)\Delta u$
44	11.0	167.0	4.9708×10^{-3}
45	11.25	130.1	4.9375×10^{-3}
46	11.50	101.3	1.7187×10^{-3}
47	11.75	78.9	2.6564×10^{-3}
48	12.00	61.4	1.1628×10^{-3}
49	12.25	47.9	1.3074×10^{-3}
50	12.50	37.3	5.1720×10^{-4}
51	12.75	29.0	3.3158×10^{-4}
52	13.00	22.6	2.8618×10^{-4}
53	13.25	17.6	4.8196×10^{-5}
54	13.50	13.7	1.1940×10^{-4}
55	13.75	10.68	5.6173×10^{-5}
56	14.00	8.32	1.6846×10^{-5}
57	14.25	6.48	1.3368×10^{-6}
58	14.50	5.04	8.9927×10^{-7}
59	14.75	3.93	9.4233×10^{-7}
60	15.00	3.06	2.9062×10^{-7}
61	15.25	2.38	8.4601×10^{-8}
62	15.50	1.86	1.6601×10^{-8}
63	15.75	1.44	2.8681×10^{-9}
64	16.00	1.125	3.7852×10^{-10}
65	16.25	0.876	7.1949×10^{-11}
66	16.50	0.683	3.5829×10^{-11}
67	16.75	0.532	2.1580×10^{-12}
68	17.00	0.414	1.3690×10^{-13}
69		0.0	8.2748×10^{-15}

Table II

Descriptions of Proportional Counter Detectors

	1 atm H_2	2.63 atm H_2*	5 atm H_2	2.63 atm CH_4	5 atm CH_4*
Inside Diameter	2.46 cm	2.23 cm	2.46 cm	2.46 cm	2.23 cm
Body Length	12.7 cm	11.43 cm	12.7 cm	12.7 cm	11.43 cm
Center Wire Diameter	25.4 μm	25.4 μm	25.4 μm	25.4 μm	25.4 μm
Sensitive Length	7.62 cm	7.62 cm	7.62 cm	7.62 cm	7.62 cm
Field Tube Diameter	127.0 μm	127.0 μm	127.0 μm	127.0 μm	127.0 μm
Field Tube Lengths	2.38 cm	1.9 cm	2.38 cm	2.38 cm	1.9 cm
Sensitive Volume	36.7 cm^3	29.73 cm^3	36.7 cm^3	36.7 cm^3	29.73 cm^3
H_2 Pressure	76 cm Hg	200 cm Hg	380 cm Hg		
CH_4 Pressure	4 cm Hg	20 cm Hg	19 cm Hg	200 cm Hg	380 cm Hg
N_2 Pressure	4 cm Hg	10 cm Hg	19 cm Hg	10 cm Hg	19 cm Hg
Stainless Steel Body	40.6 μm Thick	76.2 μm Thick	40.6 μm Thick	40.6 μm Thick	76.2 μm Thick
Resolution[a]	~5% FWHM	~5%FWHM	~6% FWHM	~6% FWHM	~8% FWHM
Minimum Energy	68 keV	120 keV	170 keV	280 keV	440 keV
Maximum Energy	350 keV	450 keV	620 keV	970 keV	2000 keV

[a] Full width at half maximum resulting from $^{14}N(n,p)^{14}C$ reaction at 585 keV.

*Detectors used in pulse shape discrimination measurements.

Table III

Benchmark Spectrum Adjustment by Measurements

Group	Adjustment Factor	
1	none	
2	1.192	
3	0.929	
4	1.134	
5	0.988	by ^{6}Li
6	1.014	
7	1.022	
8	1.242	
9	1.140	
10	1.039	
11	0.955	
12	0.967	
13	0.966	
14	0.934	
15	0.977	by Proton Recoil
16	1.017	
17	1.098	
18	1.011	
19	1.015	
20	0.852	
21	0.918	
22	0.987	
23	1.173	
24	0.946	by ^{6}Li
25	1.111	
26	1.113	
27	1.021	

Table IV

Ratios of Measured-to-Calculated Reaction Rates
for Three Forms of CFRMF Spectrum

Reaction	Benchmark	Measurements Adjusted	SAND II Adjusted	Semi-Empirical Adjusted
$^{6}Li(n,\alpha)^{3}H$	0.873	.8767	[a] 0.9403	[a] 0.9140
$^{10}B(n,\alpha)^{7}Li$	1.0934	1.1024	[a] 1.0736	[a] 1.0531
$^{235}U(n,f)F.P.$	1.00(1.58791)*	1.00(1.58713)*	1.00(1.6249)*	1.00(1.62846)*
$^{239}Pu(n,f)F.P.$	1.0446	1.0466	[a] 1.0468	[a] 1.0672
$^{237}Np(n,f)F.P.$	1.0348	.9998	[a] 0.9795	[a] 1.02214
$^{238}U(n,f)F.P.$	1.1164	1.0581	[a] 0.9743	[a] 0.9777
$^{238}U(n,\gamma)^{239}U$	0.786	0.7915	0.7628	0.70951
$^{45}Sc(n,\gamma)^{46}Sc$	1.189	1.1988	1.1741	[a] 1.0958
$^{58}Fe(n,\gamma)^{59}Fe$	1.0207	1.0270	0.9944	[a] 0.9980
$^{59}Co(n,\gamma)^{60}Co$	1.0948	1.0984	1.0384	[a] 1.0326
$^{115}In(n,\gamma)^{116m}In$	0.9526	0.9570	0.9395	0.8962
$^{197}Au(n,\gamma)^{198}Au$	1.050	1.0551	[a] 1.0142	[a] 1.0158

Table IV (Continued)

Reaction	Benchmark	Measurements Adjusted	SAND II Adjusted	Semi-Empirical Adjusted
$^{27}Al(n,p)^{27}Mg$	1.000	0.9516	[a] 0.9302	[a] 1.0053
$^{27}Al(n,\alpha)^{24}Na$	0.972	0.9228	[a] 0.8943	[a] 1.0136
$^{46}Ti(n,p)^{46}Sc$	1.235	1.1741	1.1586	1.2455
$^{47}Ti(n,p)^{47}Sc$	0.8993	0.8655	0.7962	0.83107
$^{48}Ti(n,p)^{48}Sc$	1.659	0.9550	1.5716	1.7282
$^{54}Fe(n,p)^{54}Mn$	1.0769	1.0372	[a] 0.9679	[a] 1.0309
$^{58}Ni(n,p)^{58}Co$	1.1159	1.0697	[a] 0.9955	[a] 1.0498
$^{115}In(n,n')^{115m}In$	1.1636	1.1029	[a] 1.0303	[a] 1.0354
$^{63}Cu(n,\gamma)^{64}Cu$	0.9799	0.9859	0.9523	[a] 0.996

[a] Reactions used to adjust the benchmark spectrum.

* Calculated spectral averaged cross section ($\bar{\sigma}$) value.

Figure Captions

1. CFRMF benchmark spectrum calculated by transport theory (SCAMP) using ENDF/B Version III cross sections.

2. Comparison of benchmark spectrum (SCAMP, S_8P_1) with Monte Carlo (RAFFLE) calculations for the CFRMF spectrum.

3. Comparison of benchmark spectrum (SCAMP, S_8P_1) with resonance theory (RABBLE) calculations of the CFRMF spectrum.

4. Comparison of benchmark spectrum with proton recoil measurements in CFRMF.

5. Sketches of the ^6Li detector assemblies used in the CFRMF ^6Li spectrometry measurements.

6. Comparison of benchmark spectrum with 2π geometry ^6Li spectrometry measurements in CFRMF.

7. Comparison of CFRMF benchmark spectrum with the spectrum adjusted by SAND II and the Semi-Empirical Model using measured reaction rates and ENDF/B Version IV dosimetry cross sections.

8. Comparison of CFRMF benchmark spectrum with the spectrum adjusted by proton recoil and ^6Li spectrometry measurements.

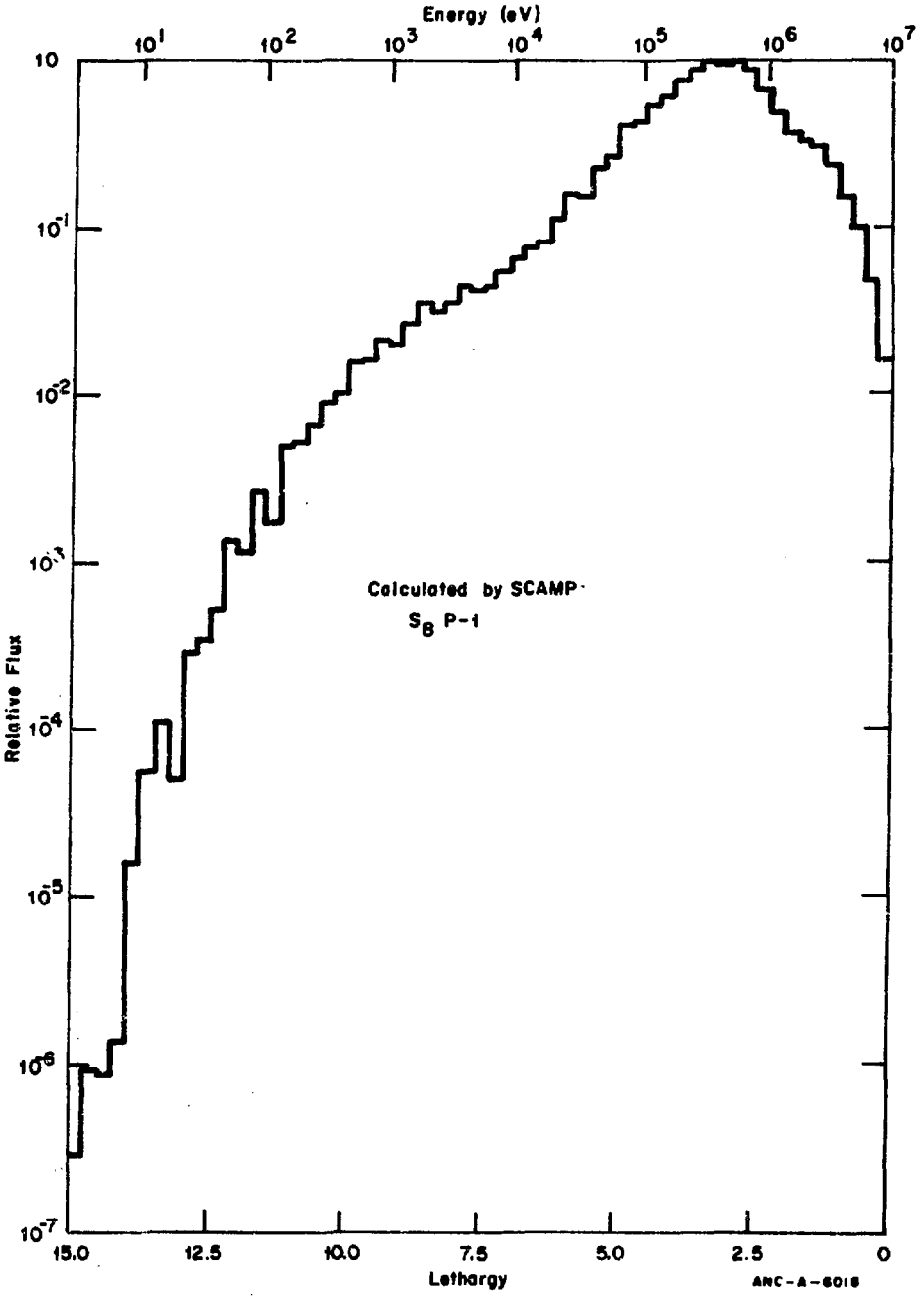

Figure 1. CFMRF benchmark spectrum calculated by transport theory (SCAMP) using ENDF/B Version III cross sections.

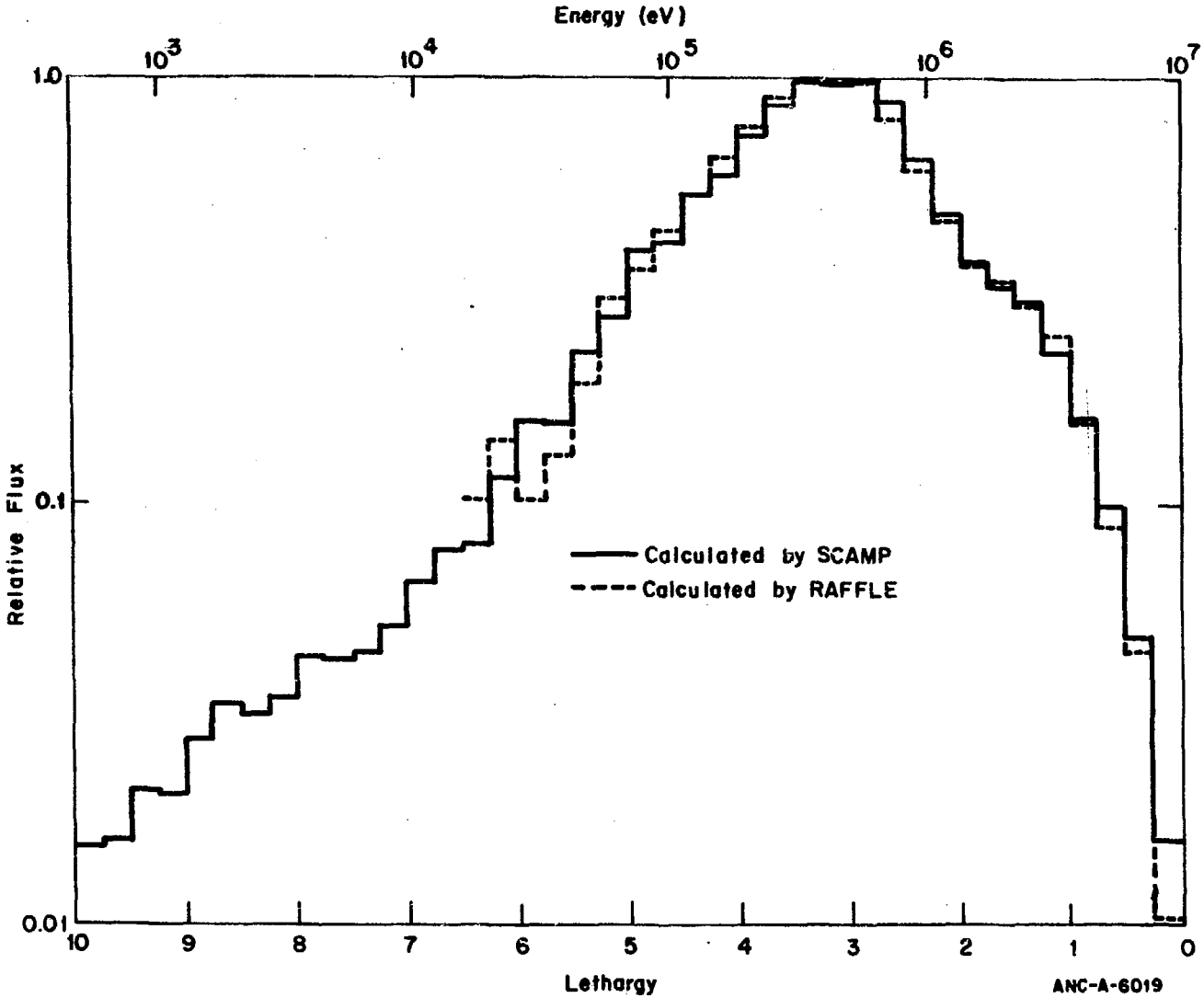

Figure 2. Comparison of benchmark spectrum (SCAMP, S_8 P_1) with Monte Carlo (RAFFLE) calculation for the CFRMF spectrum.

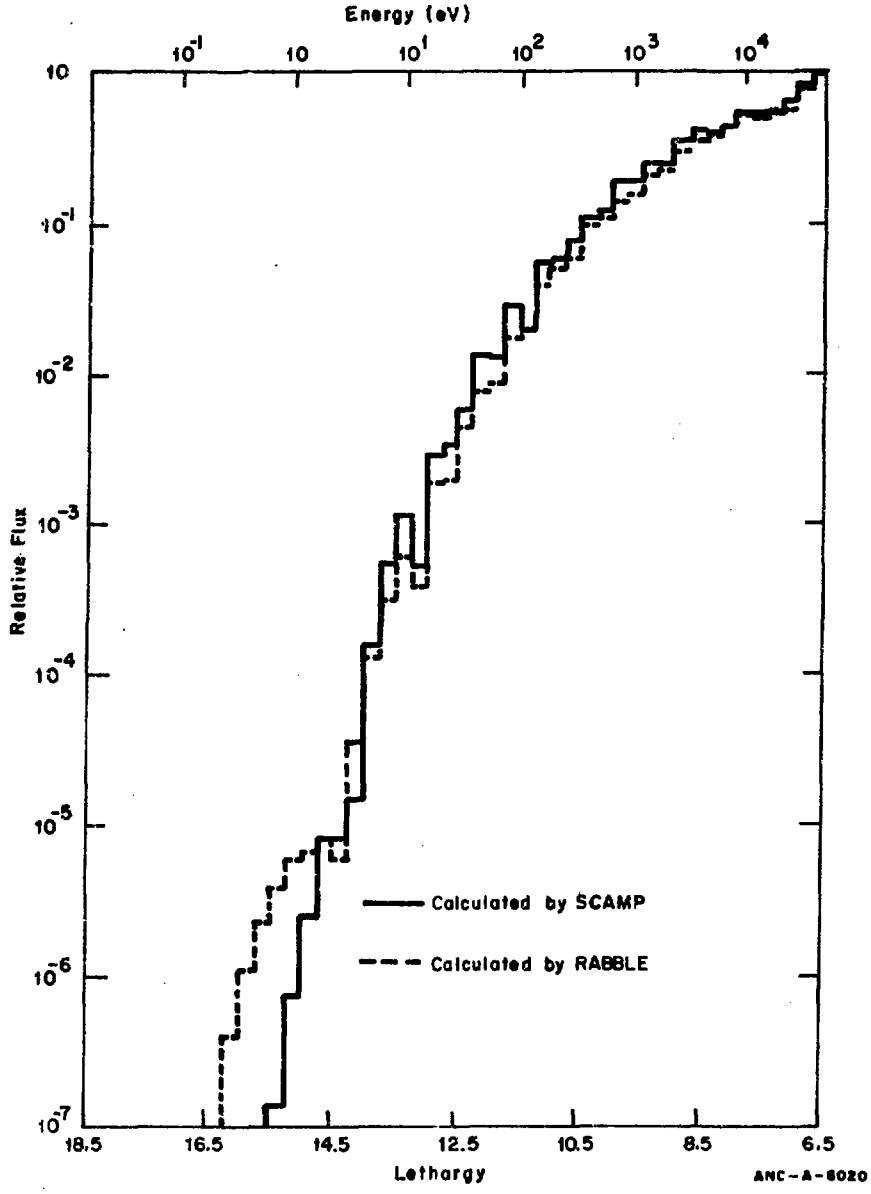

Figure 3. Comparison of benchmark spectrum (SCAMP, S_8 P_1) with resonance theory (RABBLE) calculation for the CFRMF spectrum.

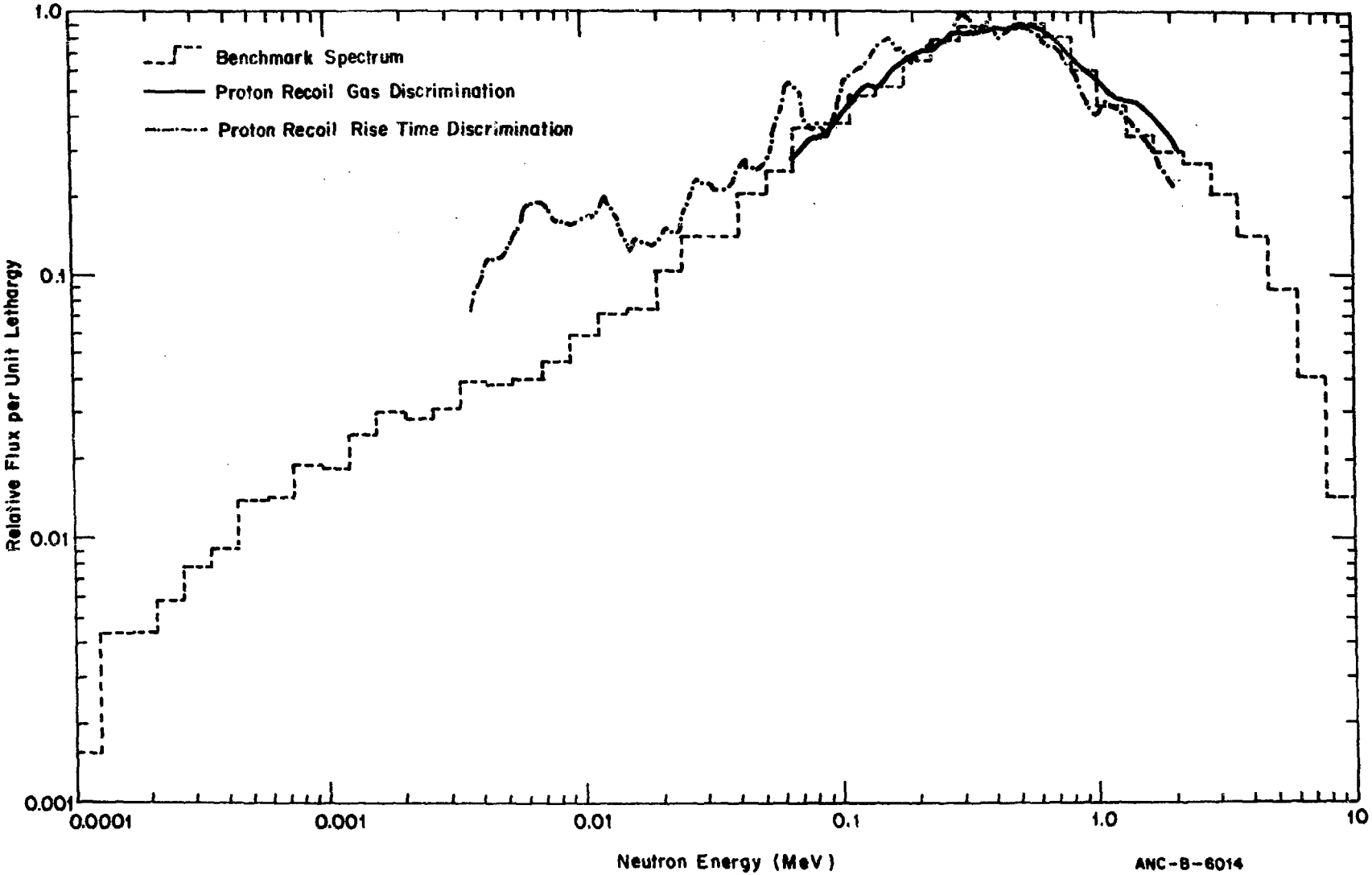

Figure 4. Comparison of benchmark spectrum with proton recoil measurements in CFRMF.

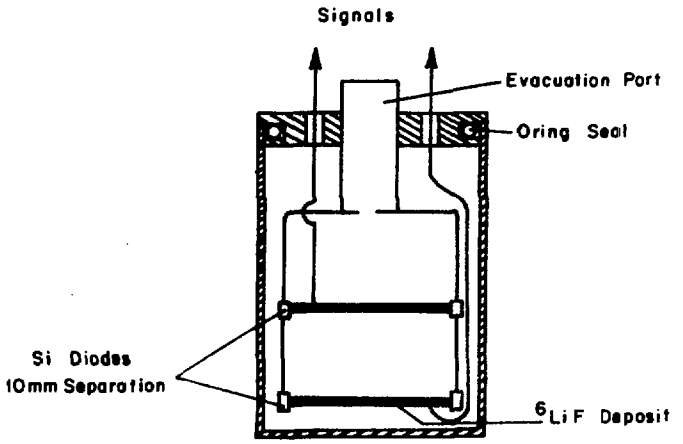

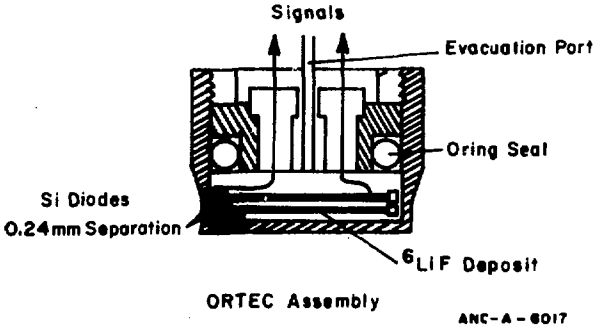

Figure 5. Sketches of the ^{6}Li detector assemblies used in the CFRMF ^{6}Li spectrometry measurements.

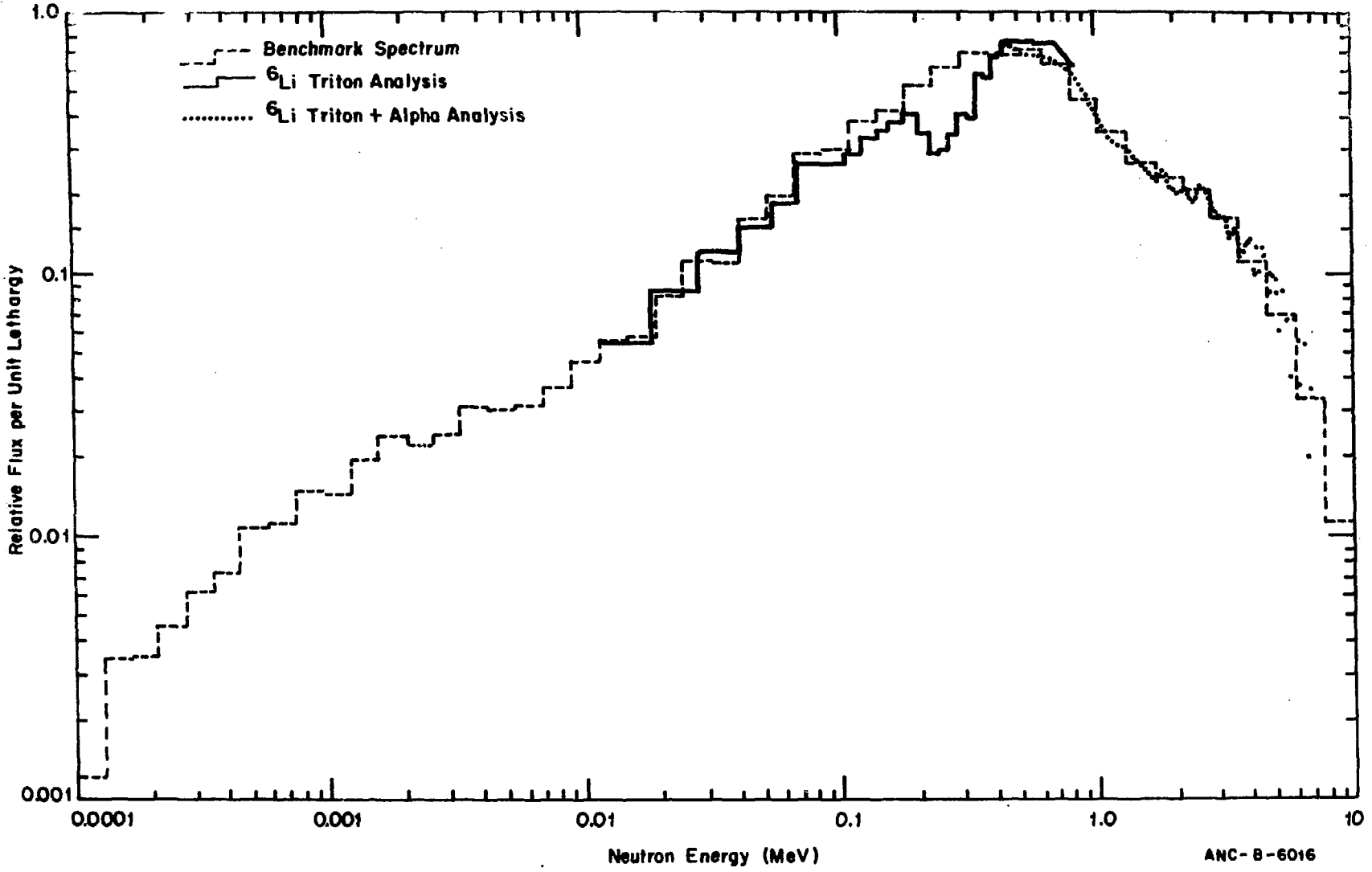

Figure 6. Comparison of benchmark spectrum with 2π geometry ^{6}Li spectrometry measurements in CFRMF.

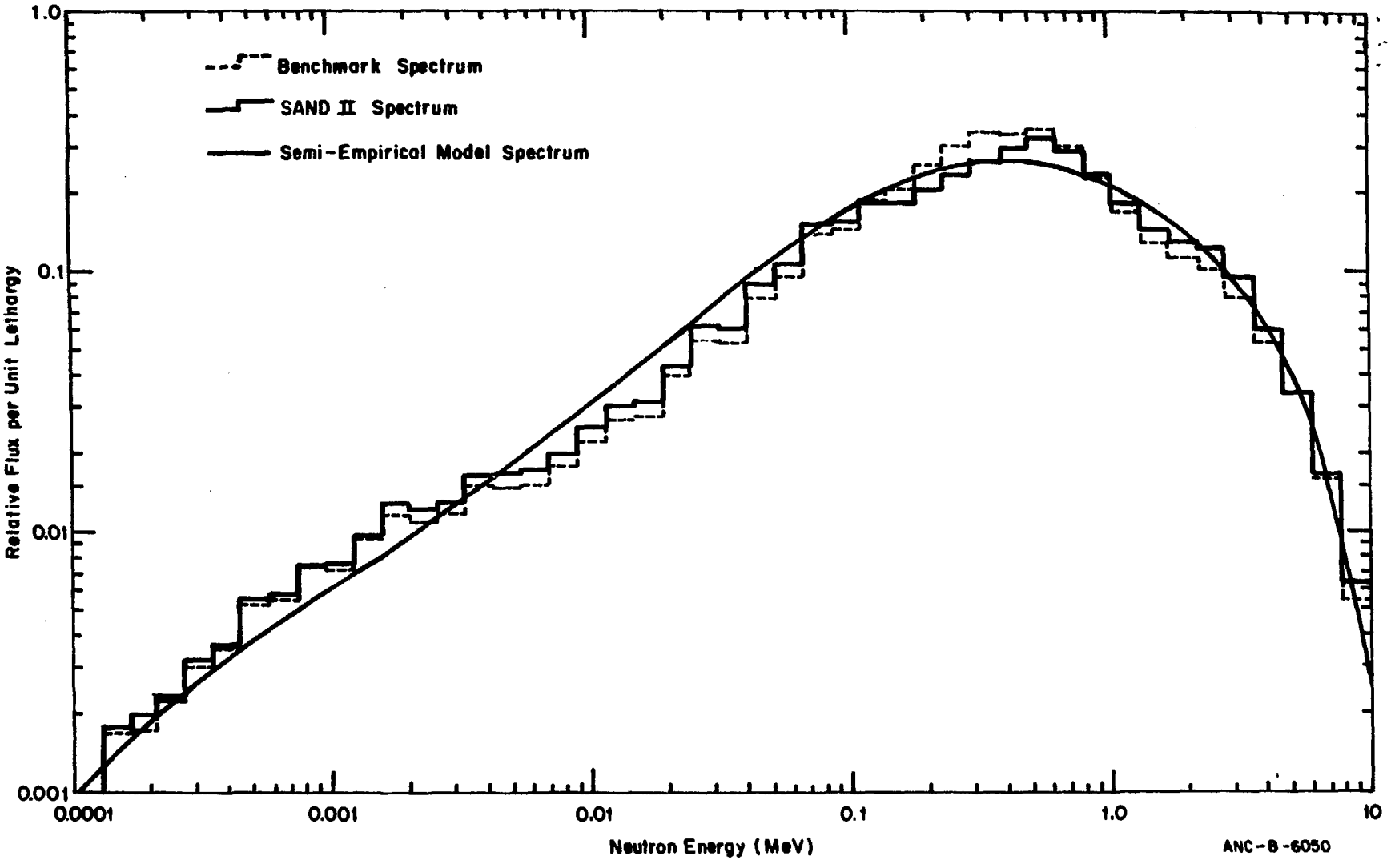

Figure 7. Comparison of CFRMF benchmark spectrum with the spectrum adjusted by SAND II and the Semi-Empirical Model using measured reaction rates and ENDF/B Version IV dosimetry cross-sections.

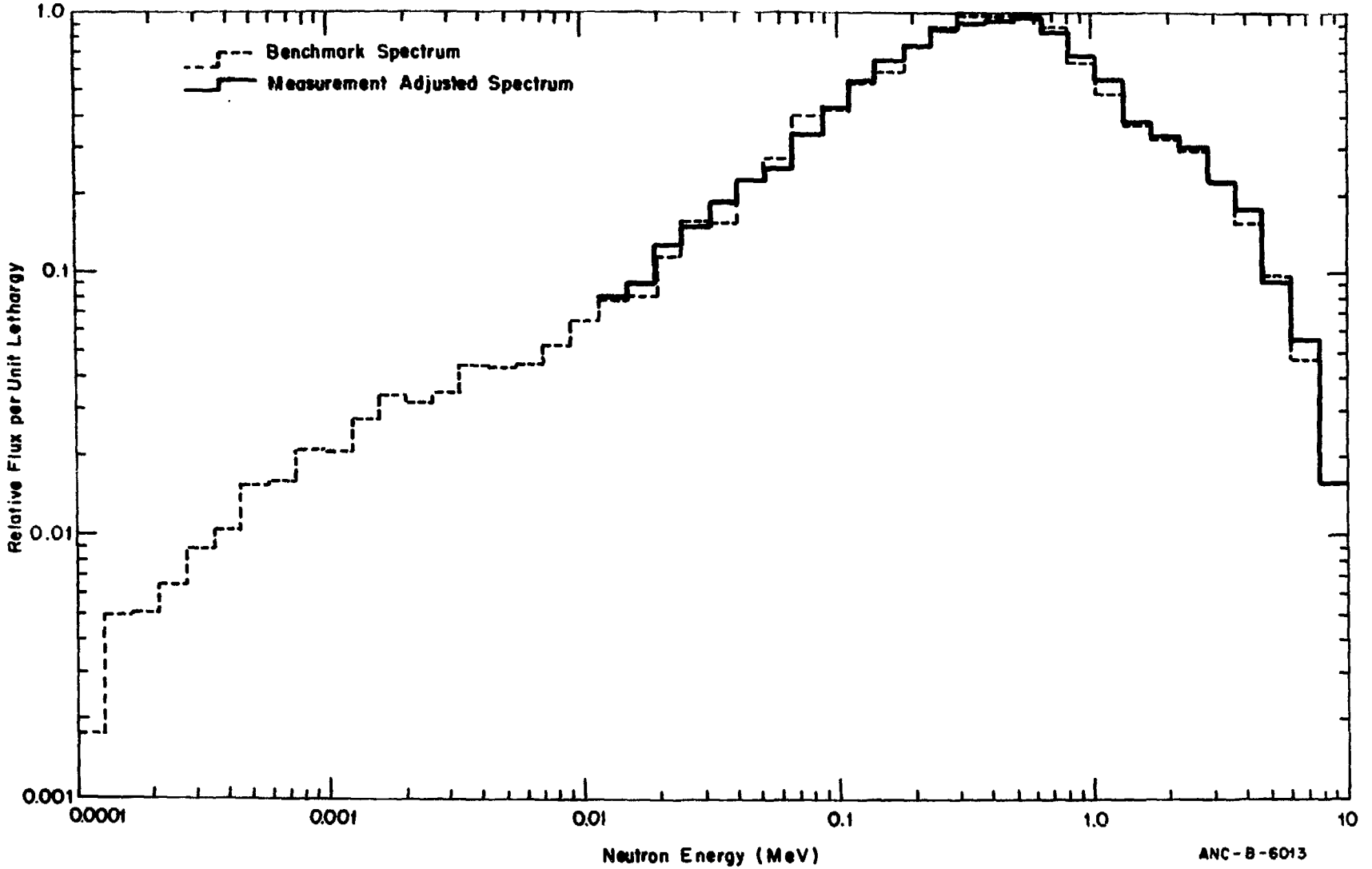

Figure 8. Comparison of CFRMF benchmark spectrum with the spectrum adjusted by proton recoil and ^{6}Li spectrometry measurements.